Available online at www.sciencedirect.com
ScienceDirect
Applied Catalysis B: Environmental 79 (2008) 334–340
APPLIED CATALYSIS B: ENVIRONMENTAL
www.elsevier.com/locate/apcatb

Photocatalytic activity of $AgBr/TiO_2$ in water under simulated sunlight irradiation

Yujing Zang, Ramin Farnood *

Department of Chemical Engineering and Applied Chemistry, University of Toronto, 200 College Street, Toronto, Ontario, Canada M5S 3E5

Received 23 January 2007; received in revised form 8 October 2007; accepted 10 October 2007
Available online 25 October 2007

Abstract

In this paper, the synthesis of $AgBr/TiO_2$ catalyst and the photocatalytic activity in water under simulated sunlight irradiation were studied. The influence of AgBr content in catalyst and the incident light intensity on the degradation of methyl orange (MO) was investigated. It was found that the initial reaction rate constant was dependent on the relative levels of AgBr content and incident light intensity, ranging between 0.008 min^{-1} and 0.023 min^{-1}. At higher levels of AgBr content (>9 wt%), MO degradation was exclusively dependent on the incident light intensity, which implied that the excessive AgBr in catalyst had negligible effect on catalyst activity. However, at lower AgBr contents, the reaction rate increased with the increase of incident light intensity, and eventually reached a plateau level, indicating that the degradation of MO was limited by AgBr content. The results from powder X-ray diffraction (XRD) analysis showed that more than 80% of AgBr remained intact after 14 h of irradiation, although metallic silver was also detected.

Keywords: Photocatalysis; $AgBr/TiO_2$ catalyst; Simulated sunlight irradiation; Advanced oxidation technology (AOT); Methyl orange

1. Introduction

Advanced oxidation technologies (AOTs) are widely used for environmental remediation of toxic organic pollutants from the domestic use and industrial activities. AOT is characterized by the generation of highly reactive radicals which can initiate the oxidative degradation of organic pollutants. One of such applications is photocatalysis in the presence of metal oxide semiconductors. TiO_2 is the most widely studied photocatalyst due to its efficiency, low cost, non-toxicity, and high stability. In this process, ultraviolet (UV) light ($\lambda < 385$ nm) is required to overcome the band gap of TiO_2 to produce electron (−)/hole (+) pairs. However, the generation of UV photons is relatively expensive and requires special equipments. Therefore, it is advantageous to use solar radiation as an abundant and inexpensive light source for photocatalysis.

In solar spectrum, however, UV radiation accounts for only about 4%, compared to more than 50% for the visible light. It was found that TiO_2 could exhibit photocatalytic activity for appropriate dyes degradation under visible light irradiation [1,2] via a self-sensitization process. In this process, the dye molecules absorb the visible light to reach an excited state. The electron is then injected from the excited dye into TiO_2 conduction band to yield the oxidizing species, which are presumed to be responsible for the dye degradation, by reducing molecular oxygen on TiO_2 surface. As a result, the absorbance of dye would be changing in the major absorption band and the corresponding wavelength would be shifting with the irradiation time. However, the self-photosensitization process is only applicable to a limited number of organic dyes. Therefore, there is a need to develop a universal photocatalyst that utilizes visible light as energy source.

One method for visible light photocatalysis is to extend the photoresponse of TiO_2-based materials to the visible region by non-metal or transition metal ions doping of TiO_2. Ho et al. [3] synthesized a catalyst by doping sulfur atoms into the lattice of anatase TiO_2 that can efficiently degrade 4-chlorophenol under visible light irradiation. The photocatalytic oxidation of toluene in gas phase over N-doped TiO_2 powders was studied [4] and it was found that more than 80% of toluene was mineralized to CO_2 and H_2O under visible light irradiation. In another work [5], the researchers developed a simple method to prepare

* Corresponding author. Tel.: +1 416 9467525; fax: +1 416 9788605.
E-mail address: ramin.farnood@utoronto.ca (R. Farnood).

0926-3373/$ – see front matter © 2007 Elsevier B.V. All rights reserved.
doi:10.1016/j.apcatb.2007.10.019

N-doped TiO_2 polycrystalline powder by calcination of the hydrolysis product of tetrabutyl titanate with ammonia solution and found that the absorption spectrum of TiO_2 shifted to a lower energy (higher wavelength) region. A Pd/$InVO_4$-TiO_2 thin film was recently synthesized by Ge and Xu [6] via a sol–gel method from the Pd and $InVO_4$ co-doped TiO_2 sol. In this catalyst, the electron could be injected from the conduction band of $InVO_4$ to the valence band of TiO_2 by absorbing energy that is lower than that of each of the individual metal oxides. In this process, Pd could act as electron trap and acceptor facilitating the electron-hole separation and electron transfer to catalyst surface. Other doping atoms investigated include carbon [7], fluorine [8], chromium [9], iron [10], just to name a few.

Developing novel catalyst material that is active under sunlight irradiation is another approach in recent years. One interesting achievement is the use of AgBr as photoactive component in the catalyst. AgBr is one of the primary materials used in the photographic industry. This compound absorbs photons in the visible light range to generate electron and hole pairs. The electrons subsequently associate with interstitial silver ions to form silver atoms in a reversible process. However, silver clusters ($\geq$3 atoms) are stable and can serve as the catalytic center for the reduction of silver ions under continuous irradiation. AgBr is thus unstable in pure crystal form. This process can be shown by Eqs. (1)–(3) [11].

$$\mathrm{AgBr} + h\nu \rightarrow \mathrm{AgBr}\,(\mathrm{h}^+ + \mathrm{e}^-) \quad (1)$$

$$\mathrm{e}^- + \mathrm{Ag}_i^+ \rightarrow \mathrm{Ag}_i^0 \quad (\mathrm{Ag}_i^+ : \text{interstitial silver ions}) \quad (2)$$

$$\mathrm{AgBr} \xrightarrow{h\nu} \mathrm{Ag} + \tfrac{1}{2}\mathrm{Br}_2 \quad (3)$$

However, AgBr could maintain its stability and photocatalytic activity if it is dispersed on certain support materials. Kakuta et al. [12] prepared AgBr/SiO_2 catalyst from Schumann emulsion for photolysis of CH_3OH/H_2O solution under UV illumination. The generation of H_2 was continued for 200 h without destruction of AgBr although metallic silver was detected from XRD analysis. AgBr/Al-MCM-41 catalyst was synthesized and applied for gas-phase decomposition of CH_3CHO under both visible light and UV irradiation [13]. AgBr together with metallic silver that was generated during synthesis and irradiation processes, were thought to be the photoactive species, and the fine dispersion of AgBr on high-surface-area silica was suggested to be essential for the photocatalytic effects. Another catalyst is Ag/AgBr/TiO_2 prepared by Hu et al. [14] to destroy azodyes and inactivate *E. coli* in water under visible light irradiation. They found that the catalyst activity for azodyes decomposition was maintained effectively after successive cycling runs without the destruction of AgBr. From electron spin resonance (ESR) analysis and H_2O_2 measurement, they found that $^{\bullet}OH$ or $O_2^{-\bullet}$ radicals were produced in the visible light illuminated aqueous Ag/AgBr/TiO_2 suspension. Hu et al. suggested that Ag^0 species formed from synthesis and irradiation processes could scavenge the positive holes (h^+) and then trap electrons to prevent AgBr from decomposition. In their work, however, catalyst containing only one level of AgBr was prepared and studied for its photoactivity, stability and possible reaction mechanism. The influences of experimental parameters were not reported.

In the present study, catalysts with several levels of AgBr contents on TiO_2 were synthesized, and methyl orange (MO) was chosen as a model organic compound to evaluate catalyst activity under simulated sunlight illumination in water. The influences of AgBr content and incident light intensity on MO degradation efficiency were investigated from the mineralization process.

2. Experimental work

2.1. Materials

TiO_2 (Degussa, type P25, 70% anatase, 30% rutile, average particle size of 21 nm, specific surface area of 50 m^2/g) was used as received. Methyl orange, cetylmethylammonium bromide (CTAB), silver nitrate ($AgNO_3$), ammonium hydroxide, *N*,*N*-diethyl-*p*-phenylenediamine sulfate salt (DPD), and concentrated nitric acid (70%) were purchased from Sigma–Aldrich.

2.2. Catalyst synthesis

AgBr/TiO_2 catalysts were synthesized using the deposition–precipitation method. A 10 g/L TiO_2 aqueous suspension was prepared and sonicated for 30 min, followed by the addition of certain amount of CTAB to the suspension and stirring magnetically for another 30 min. The complex solution of $AgNO_3$ in ammonia hydroxide (28–30 wt% of NH_3) was then added, and the mixture was heated and maintained at 80–90 °C for 18 h. The amount of $AgNO_3$ was adjusted to obtain the desired level of AgBr in the catalyst. The molar ratio of NH_3/Ag^+ was around 6 in the complex solution. Bromide ion (from CTAB) was present in excess amounts to effectively precipitate AgBr from $Ag(NH)_n^+$ complex solution. The suspension was centrifuged and washed with water and the remaining solid paste was dried at 90 °C overnight and then calcined at 500 °C for 3 h. For comparison, a blank catalyst containing only TiO_2 was also prepared. The procedure for the blank catalyst synthesis was same as described above except that no $AgNO_3$ was added to the ammonia hydroxide solution.

Ag/TiO_2 catalysts were also prepared using the photodeposition method [15]. Certain amount of TiO_2 was added into $AgNO_3$ aqueous solutions containing different levels of Ag^+. The suspensions were illuminated for 60 min under UV light using the irradiation system described in Section 2.4. The suspension was centrifuged, washed with water and the solid was dried for 24 h at 90 °C.

2.3. Catalyst characterization

The crystal phase of synthesized AgBr/TiO_2 catalyst was analyzed by powder X-ray diffraction (XRD) pattern using a Siemens D5000 θ/2θ diffractometer with Cu-Kα radiation

(λ = 1.5418 nm) at 50 kV and 35 mA. AgBr was digested from catalysts using concentrated nitric acid for Ag quantification by Inductively Coupled Plasma Atomic Emission Spectrometry (ICP-AES) (PerkinElmer Model Optima 3000DV ICP AEOS). The BET specific surface area of catalyst was obtained on a Coulter SA 3100 area and pore size analyzer. The particle size in the suspension was measured by Beckman Coulter Multisizer™ 3. The UV–Vis absorption spectrum of catalyst was recorded on a PerkinElmer Lambda 35 spectrophotometer with an integrating sphere attachment for the diffuse reflectance in the range of 220–600 nm. X-ray photoelectron spectroscopy (XPS) spectra were obtained on a Leybold (Specs) MAX 200 XPS system (Specs GmbH, Berlin, Germany) utilizing an unmonochromatised Mg-Kα source operating at 15 kV and 20 mA. The energy range was calibrated against Cu 2p3/2 and Cu 3p lines at 932.7 and 75.1 eV, respectively, with the main hydrocarbon peak shifted to 285.0 eV to account for energy changing correction.

2.4. Photocatalytic activity

The photoactivity of catalyst was examined by the degradation of methyl orange in a 60-mL cylindrical batch reactor. The light source was a 1000 W xenon arc lamp installed in a laboratory lamp housing system (Oriel) to simulate the solar radiation. Light passed through a lens assembly, a water filter, a beam turner, and a UV cutoff filter (>420 nm) before entering the reactor. Three levels of incident light intensity were applied in this study by adjusting the power supply connected to the lamp housing. The incident light intensity on the surface of reaction medium was measured using a miniature fiber optic spectroradiometer (USB2000, Ocean Optics Inc.), and the values were 9.2, 11.8 and 19.1 W/m^2 (395–500 nm). The cylindrical reactor was placed in a water tank at room temperature. In a typical experiment, 50 mL of the reaction suspension containing catalyst and MO was transferred to the reactor and was illuminated for a certain period of time. Since the main purpose of this study is to assess the activity of photocatalyst at various AgBr/TiO_2 ratios under simulated sunlight irradiation, the catalyst loading in the suspension and the initial concentration of MO was kept constant at 2.5 g/L and 15 mg/L, respectively, for all runs. Two samples were collected at each given irradiation time interval. Filtered samples were analyzed using the UV-Vis spectrophotometer to monitor the degree of MO photodegradation. MO concentration was determined from the absorbance at a wavelength of 465nm. The experimental errors (standard deviation, S.D.) were found to be lower than 3%. For comparison, the blank catalyst (only TiO_2) and Ag/TiO_2 catalysts were also studied for MO degradation under the same experimental conditions. In order to ascertain the generation of hydrogen peroxide in the reaction medium, the catalyst suspension in the absence of MO was illuminated under the same irradiation conditions. The concentration of hydrogen peroxide was determined using DPD method [16,17].

3. Results and discussion

3.1. Characterization of AgBr/TiO_2 photocatalysts

The physical properties of synthesized catalysts are listed in Table 1. The synthesized catalysts had BET surface areas from 31.9 m^2/g to 45.1 m^2/g. The particle sizes of all catalysts in reaction media were around 4.5 μm. From XPS analysis, the concentrations of Ag and Br species in the synthesized catalysts were up to 1.6 at.% and 1.0 at.%, respectively, which indicated that the surface of TiO_2 was not completely covered by AgBr. The weight percentage of (Ag + Br) was calculated based on the atomic concentrations of all the elements (C, O, Ti, Br and Ag) determined by XPS analysis on catalyst surface. From Table 1, AgBr content did not increase proportionally to $AgNO_3$ amount during the catalyst preparation. In fact, regression analysis showed that increasing the amount of $AgNO_3$ by a factor of 2 during catalyst preparation resulted in only 25% increase of the AgBr content on catalyst surface with a R^2 of 0.87. The UV–Vis absorption spectrum of catalyst TD was measured and shown in Fig. 1. For comparison, the spectra of TiO_2 and Ag/TiO_2 catalyst were also displayed. Both AgBr/TiO_2 and Ag/TiO_2 catalysts exhibited absorption in the visible light range (400–600 nm).

The XRD patterns of catalyst TD before and after photolysis are shown in Fig. 2. Initially, in addition to the common anatase and rutile phases of TiO_2, only AgBr peaks were present in XRD pattern of the fresh catalyst, whereas after 1 h irradiation a new peak attributed to metallic silver (0.45 wt%) was appeared, which indicated that only 8% of AgBr was converted to Ag after 1 h illumination.

Table 1
Physical properties of synthesized catalysts

Catalyst	$AgNO_3/TiO_2$ (wt%)	BET surface area (m^2/g)	AgBr content[a] (wt%)	XPS analysis		
				Ag (at.%)	Br (at.%)	(Ag + Br) content[b] (wt%)
TA	0	–	–	–	–	–
TC	10.0	45.1	4.77	–	–	–
TD	17.5	–	7.85	1.0	0.8	8.37
TE	21.0	37.7	9.57	1.4	0.8	10.07
TF	25.0	–	11.56	1.2	0.9	10.25
TG	35.0	31.9	13.79	1.6	1.0	11.80

[a] Based on ICP-AES analysis.
[b] Calculated values based on all elements.

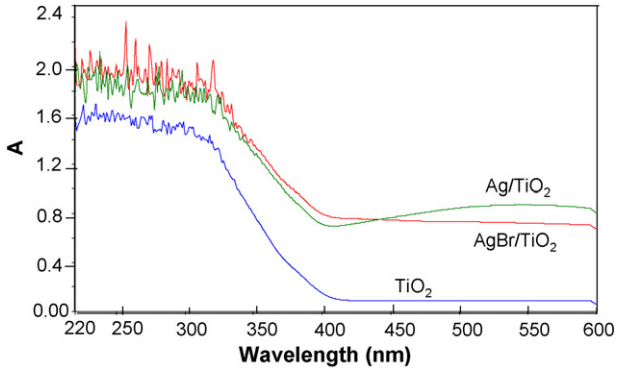

Fig. 1. UV–Vis spectra of catalysts $AgBr/TiO_2$ (TD), TiO_2 and Ag/TiO_2.

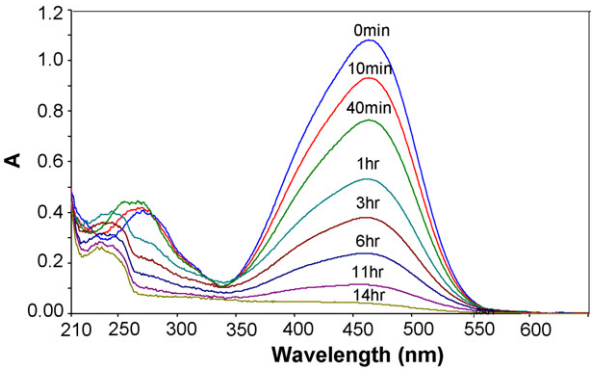

Fig. 3. Spectra of MO during degradation process using catalyst TD. (11.8 W/m^2 of incident light intensity, 50 mL of suspension, 15 mg/L of $[MO]_0$, 2.5 g/L of catalyst loading).

3.2. $AgBr/TiO_2$ photocatalysis

Before evaluating the photocatalytic activity of $AgBr/TiO_2$, two control experiments were carried out: (i) the direct photolysis of MO in the absence of catalyst and (ii) the decomposition of MO in catalyst suspension in the absence of light source. The results showed that no decomposition of MO occurred under these conditions. However, due to adsorption to catalyst surface, the concentration of MO decreased by 5%–8% in the bulk solution in the absence of light source, and remained at a constant level after 60 min. Therefore, 1 h was chosen as the dark adsorption time before irradiating the reaction media in all runs.

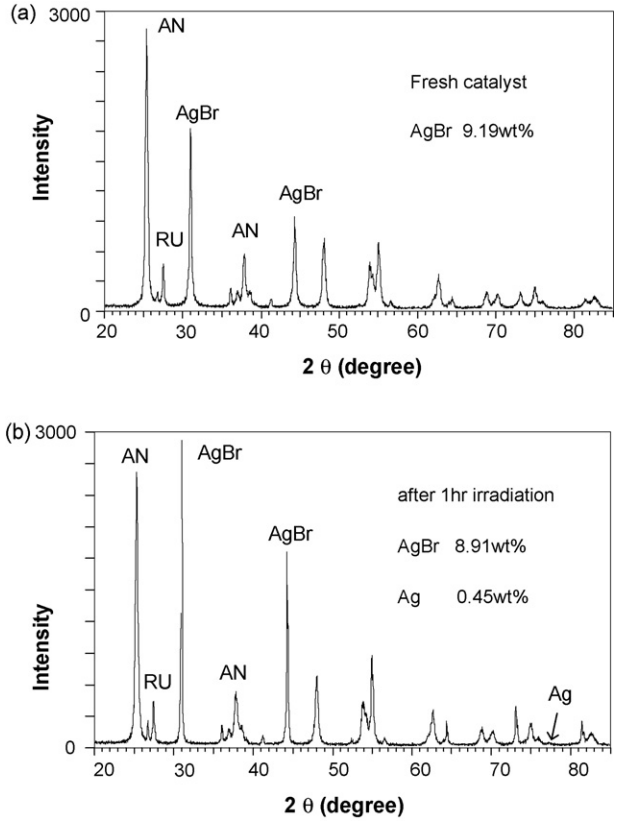

Fig. 2. XRD patterns for fresh catalyst TD (a) and after 1 h irradiation (b) (AN: anatase TiO_2, RU: rutile TiO_2).

Based on Fig. 3, more than 95% of MO was degraded in the presence of TD catalyst and simulated sunlight after 14 h irradiation. In addition, there was no maximum peak shift of MO, which indicated that the self-photosensitization process [1] did not occur under these conditions.

XRD analysis of irradiated catalyst showed that the concentrations of AgBr and metallic silver were 9.11 wt% and 1.20 wt%, respectively. This means more than 80% of AgBr remained intact after 14 h of irradiation. Earlier studies [11] reported that scavenging electrons by interstitial silver ions to form silver atoms was a reversible process. Silver cluster (Ag_2) is not stable and can react with the holes to decompose into silver ions and a conduction-band electron:

$$Ag_2 + h^+ \rightarrow Ag_2^+ \rightarrow Ag^0 + Ag_i^+ \quad (4)$$

$$Ag^0 \rightarrow Ag_i^+ + e^- \quad (5)$$

Dispersing AgBr on TiO_2 might inhibit silver atoms to form larger clusters ($\geq$3 atoms) and prevent AgBr decomposition. However, further work is required to elucidate the mechanism for AgBr stability.

3.3. Effect of AgBr content

In order to determine the optimal AgBr content in catalyst, the complete mineralization processes were conducted using catalysts with varying amounts of AgBr. Fig. 4 shows the variation of $Ln(C_0/C)$ of MO with the irradiation time. Increasing AgBr content enhanced the photoactivity of catalysts but at higher AgBr levels, catalyst activity remained unchanged. Moreover, MO degradation profiles in the presence of catalysts with high levels of AgBr (TE, TF and TG) are practically the same. Hence, the amount of AgBr that can absorb light and initiate the reaction has to be similar for these catalysts.

It is interesting to note that the initial MO degradation rates (<20 min) were the same in all runs. The percentages of residual MO for the first 120 min are summarized in Table 2. For comparison, the results using TiO_2 (TA) and Ag/TiO_2 (T-1 and T-2) catalysts are also included in this table. Based on this

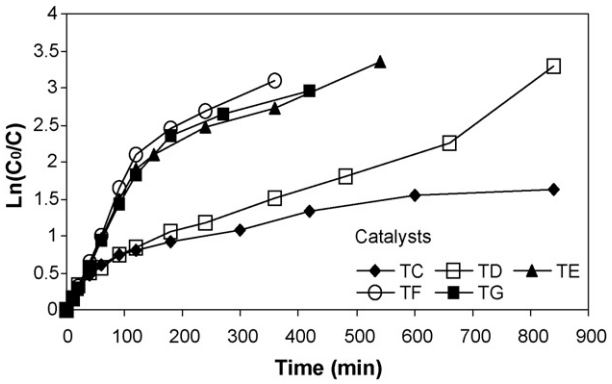

Fig. 4. Effect of AgBr content on MO degradation during complete mineralization process. (11.8 W/m^2 of incident light intensity, 50 mL of suspension, 15 mg/L of $[MO]_0$, 2.5 g/L of catalyst loading).

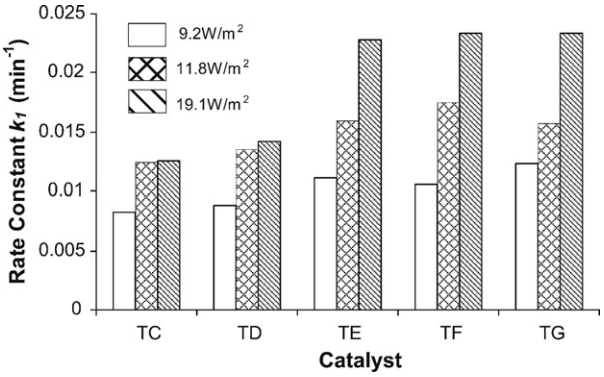

Fig. 6. The effect of incident light intensity on the initial rate constant (k_1) (50 mL of suspension, 15 mg/L of $[MO]_0$, 2.5 g/L of catalyst loading).

table, the initial reaction rate was independent of the amount of AgBr in the catalysts, and AgBr was the only photoactive component to start the photocatalytic degradation of MO under the simulated sunlight.

It has been reported [14] that H_2O_2 can be formed in the AgBr/TiO_2 suspension during the irradiation process. In this study, H_2O_2 concentration in the aqueous AgBr/TiO_2 suspensions was measured in the absence of MO after 40 min of irradiation according to the method described in the literature [16,17]. The measured H_2O_2 quantities after 40 min irradiation varied from 14.3 μM to 42.8 μM (Fig. 5) depending on catalyst, and the decomposition of MO was found to correlate well with the concentration of H_2O_2 in the catalyst suspension ($R^2 = 0.73$). For comparison, similar tests were conducted on the blank catalyst TA and two Ag/TiO_2 catalysts (T-1 and T-2). However, no H_2O_2 was detected in these experiments, which implies H_2O_2 was only formed in the presence of AgBr/TiO_2. According to the photocatalytic mechanism, H_2O_2 could be formed from $O_2^{-\bullet}$ or $^{\bullet}OH$ that are generated from the reaction of electron/holes with the adsorbed O_2/H_2O on AgBr/TiO_2 catalyst surface. This means MO destruction in the present study is dependent on the photogenerated electrons or holes or both of them; however, further investigation is required to clarify this process.

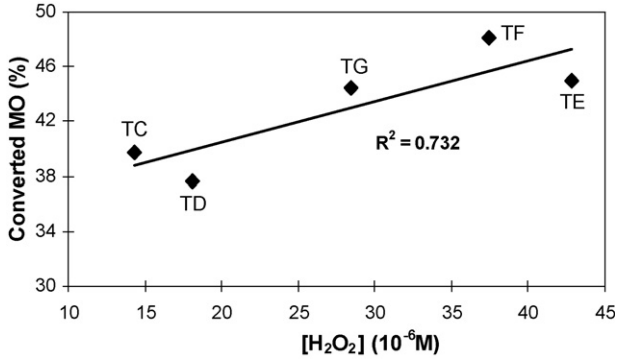

Fig. 5. Relationship between H_2O_2 concentration and MO conversion. (11.8 W/m^2 of incident light intensity, 50 mL of aqueous suspension, 2.5 g/L of catalyst loading).

3.4. Effect of visible light intensity

For catalysts with high AgBr content (TE, TF and TG), the incident light intensity is expected to be the rate-controlling parameter. In order to illustrate this effect, experiments were carried out under three levels of incident light intensity, and the *pseudo*-first-order rate constant (k_1) at the initial stage of reaction (40 min for TC and TD, and 90min for TE, TF and TG) was calculated and showed in Fig. 6. The mineralization processes at 9.2 W/m^2 and 19.1 W/m^2 of light intensity are also displayed in Figs. 7 and 8.

Based on Fig. 6, the reaction rate constant depends both on the AgBr content in catalyst and incident light intensity. At low AgBr contents (TC and TD), increasing the light intensity from 9.2 W/m^2 to 11.8 W/m^2 enhanced MO degradation, whereas further increase in light intensity to 19.1 W/m^2 only led to less than 5% improvement in the rate constant. At higher AgBr contents (TE, TF and TG), increasing light intensity steadily enhanced the reaction rate constant. Meanwhile, as discussed earlier, there was no difference in k_1 among TE, TF and TG catalysts under same level of incident light intensity. These results may be explained based on the relative amounts of AgBr and photons in the reaction system. At low AgBr loading (TC and TD), the quantity of AgBr on catalyst surface is limited while photons are present in excess amounts. Therefore, more AgBr on catalyst surface can generate more reactive species and destroy more MO to show a higher activity under the same

Table 2
MO degradation in the presence of different catalysts

Time (min)	Residual MO (%)							
	TA	TC	TD	TE	TF	TG	T-1[a]	T-2[b]
10	99.4	86.9	85.1	87.4	85.8	85.4	99.4	99.8
20	98.9	74.4	72.2	75.5	73.2	74.4	98.8	99.0
40	98.5	62.4	60.3	55.0	51.9	55.6	99.0	98.8
60	–	54.8	56.8	38.6	37.1	39.3	–	98.3
120	98.9	44.7	42.7	14.8	12.2	16.1	98.1	95.3

11.8 W/m^2 of incident light intensity, 50 mL of suspension, 15 mg/L of $[MO]_0$, 2.5 g/L of catalyst loading.

[a] T-1: Ag/TiO_2(w/w) = 0.02.

[b] T-2: Ag/TiO_2(w/w) = 0.11.

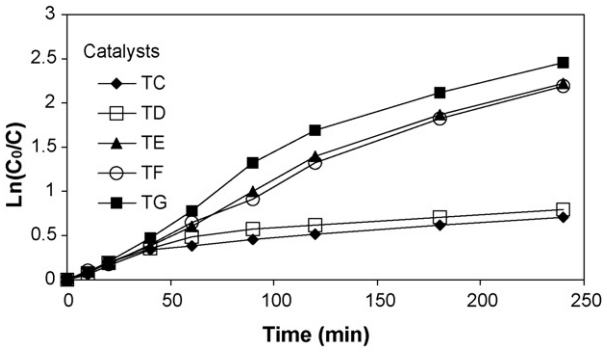

Fig. 7. MO mineralization profiles under the incident light intensity of 9.2 W/m^2 (50 mL of suspension, 15 mg/L of $[MO]_0$, 2.5 g/L of catalyst loading).

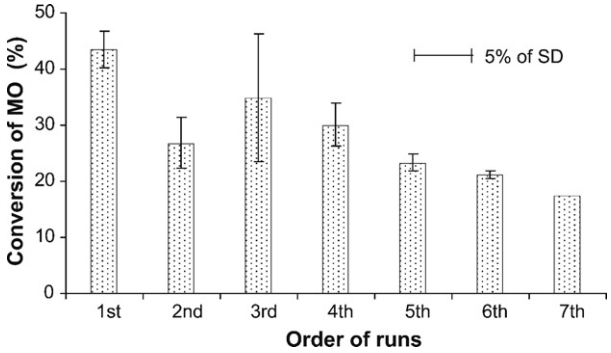

Fig. 9. Cycling runs of MO degradation in the presence of catalyst TD (11.8 W/m^{2}of incident light intensity, 50 mL of suspension, 15 mg/L of $[MO]_0$, 2.5 g/L of catalyst loading, 1 h of irradiation time).

level of incident light intensity, but the activity cannot be further enhanced with the increase of light intensity. At higher AgBr levels, AgBr is present in excess and reaction is photon-limited. Thus, catalyst activity is independent of AgBr content.

3.5. Catalyst stability

The stability of synthesized catalysts was investigated by cycling runs. The catalyst loading, irradiation time and incident light intensity were 2.5 g/L, 1 h and 11.8 W/m^2, respectively, for each cycling run. The recovery of catalyst was achieved by centrifugation to remove the bulk solution, and subsequent drying at 90 °C for 24 h (except for the second run) without any further treatment. The results displayed in Fig. 9 show that although the conversion efficiency of MO decreased after each run, the catalyst still exhibited activity after seven successive cycles under the simulated sunlight irradiation. The lower MO conversion for the second run could be due to the shorter drying time, i.e. due to higher residual moisture so that the actual catalyst loading maybe lower than the target value of 2.5 g/L. The XRD analysis showed that AgBr was still present (10.80 wt%) after the cyclic tests; however, metallic silver was increasingly formed during the reaction. The Ag^0 content was 0.45 wt%, 1.2 wt%, and 2.64 wt% after 1 h, 14 h and 7th cyclic run irradiation, respectively. Further work is required to better understand factors that affect the rate of AgBr decomposition and to improve the catalyst stability.

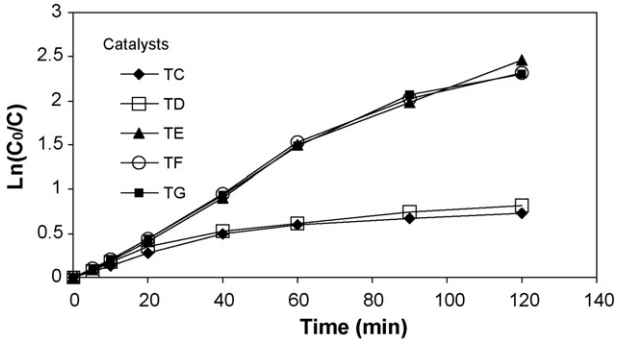

Fig. 8. MO mineralization profiles under the incident light intensity of 19.1 W/m^2 (50 mL of suspension, 15 mg/L of $[MO]_0$, 2.5 g/L of catalyst loading).

4. Conclusions

$AgBr/TiO_2$ catalyst was synthesized and evaluated in terms of the catalytic activity in water under simulated sunlight irradiation. The results of XRD analysis of the fresh/irradiated catalysts indicate that AgBr is stable although metallic silver forms during the reaction time. The investigation regarding the effects of AgBr content and incident light intensity on MO degradation indicates that the overall reaction rate depends on the relative levels of these parameters. At low AgBr levels, the degradation process is AgBr-limited, and increasing incident light intensity may not improve the reaction rate. On the other hand, excessive amount of AgBr has negligible effect on catalyst activity while increasing AgBr contents, and MO degradation rate will be photon-limited under this condition. MO degradation efficiency correlates with H_2O_2 concentration in the irradiated aqueous suspension, suggesting that $^{\bullet}OH$ or $O_2^{-\bullet}$ or both radicals are formed in this process. Although $AgBr/TiO_2$ catalyst exhibited good photocatalytic activity and stability in degrading MO, its performance may be improved by reducing particle size, better dispersion of AgBr on the catalyst surface, and doping. Further work is required to evaluate the effectiveness of this catalyst in degrading common pollutants and the reaction pathways under various catalyst loadings and pollutant concentrations.

Acknowledgments

Financial support from the Natural Sciences and Engineering Research Council of Canada (NSERC) and Canada Foundation of Innovation (CFI) is gratefully acknowledged.

References

[1] T. Wu, G. Liu, J. Zhao, J. Phys. Chem. B 102 (1998) 5845–5851.
[2] J. Zhao, C. Chen, W. Ma, Topics Catal. 35 (2005) 269–278.
[3] W. Ho, J.C. Yu, S. Lee, J. Solid State Chem. 179 (2006) 1171–1176.
[4] Y. Irokawa, T. Morikawa, K. Aoki, S. Kosaka, Phys. Chem. Chem. Phys. 8 (2006) 1116–1121.
[5] Z. Wang, W. Cai, X. Hong, X. Zhao, F. Xu, C. Cai, Appl. Catal. B: Environ. 57 (2005) 223–231.
[6] L. Ge, M. Xu, Mater. Sci. Eng. B 131 (2006) 222–229.

[7] Y. Li, D.S. Hwang, N.H. Lee, S.J. Kim, Chem. Phys. Lett. 404 (2005) 25–29.
[8] D. Li, N. Ohashi, S. Hishita, T. Kolodiazhnyi, H. Haneda, J. Solid State Chem. 178 (2005) 3293–3302.
[9] J.Y. Shi, W.H. Leng, W.C. Zhu, J.Q. Zhang, C.N. Cao, Chem. Eng. Technol. 29 (2006) 146–154.
[10] K.S. Rane, R. Mhalsiker, S. Yin, T. Sato, K. Cho, E. Dunbar, P. Biswas, J. Solid State Chem. 179 (2006) 3033–3044.
[11] C.N. Proudfoot, Handbook of Photographic Science and Engineering, second ed., IS & T, 1997.
[12] N. Kakuka, N. Goto, H. Ohkita, T. Mizushima, J. Phys. Chem. B 103 (1999) 5917–5919.
[13] S. Rodrigues, S. Uma, I.N. Martyanov, K.J. Klabunde, J. Catal. 233 (2005) 405–410.
[14] C. Hu, Y. Lan, J. Qu, X. Hu, A. Wang, J. Phys. Chem. B 110 (2006) 4066–4072.
[15] H. Tada, K. Teranishi, Y. Inubushi, S. Ito, Langmuir 16 (2000) 3304–3309.
[16] H. Bader, V. Sturzenegger, J. Hoigné, Water Res. 22 (1988) 1109–1115.
[17] T. Wu, G. Liu, J. Zhao, H. Hidaka, N. Serpone, J. Phys. Chem. B 103 (1999) 4862–4867.